Non linear properties of nitride-based nanostructures for optically controlling the speed of light at 1.5 µm

F.B. Naranjo[a,*], M. González-Herráez[a], S. Valdueza-Felip[a], H. Fernández[b], J. Solis[b] S. Fernández[c], E. Monroy[d], J. Grandal[e], M.A. Sánchez-García[e].

[a]*Departamento de Electrónica, Escuela Politécnica, Universidad de Alcalá Campus Universitario, 28871 Alcalá de Henares, Madrid, Spain.*

[b]*Instituto de Óptica, C.S.I.C., Serrano 121, 28006 Madrid, Spain.*

[c] *Departamento de Energías Renovables, Energía Solar Fotovoltaica, Centro de Investigaciones Energéticas, Medioambientales y Tecnológicas (CIEMAT), Avda. Complutense 22, 28040 Madrid, Spain*

[d]*Equipe mixte CEA-CNRS-UJF « Nanophysique et Semiconducteurs », DRFMC/SP2M/PSC, CEA-Grenoble, 17 rue des Martyrs, 38054-Grenoble cedex 9, France.*

[e]*ISOM and Departamento de Ingeniería Electrónica, ETSI Telecomunicación, Universidad Politécnica de Madrid, Ciudad Universitaria, 28040 Madrid, Spain*

Abstract

Future bandwidth demand in optical communications requires all-optical devices based on optical non-linear behaviour of materials. InN, with a room temperature direct band-gap well below 0.82 eV (1.5 µm) is very attractive for these applications. In this work, we characterize the nonlinear optical response and recombination lifetime of the interband transition of InN layers grown on GaN-template and Si(111) by molecular beam epitaxy. Non-linear characterization shows a decrease of the third order susceptibility, $\chi^{(3)}$, and an increase of recombination lifetime when decreasing the energy difference between the excitation and the apparent optical band-gap energy of the analyzed samples. Taking into account the nonlinear characterization, an optically-

*corresponding author. E-mail address: naranjo@depeca.uah.es
Phone: +34 91 885 65 58 x5 ; FAX: +34 91 885 6591

controlled reduction of the speed of light by a factor S = 4.2 is obtained for bulk InN at 1.5 μm. The *S* factor of InN (5 nm)/$In_{0.7}Ga_{0.3}N$ (8 nm) multiple quantum well heterostructures at the same operation wavelength is analysed, predicting an increase of this factor of three orders of magnitude. This result would open the possibility of using InN-based heterostructures for all-optical devices applications.

KEYWORDS: InN, nonlinear optics, four wave mixing, slow light.

1. Introduction.

In the last years, there has been an increasing demand of higher optical bandwidth and transparency in optical networks. The main challenge to satisfy this demand lies in the network nodes themselves, since the electronic processing of information in these nodes is inherently bandwidth-limited and not transparent to the data format. Therefore, these nodes should evolve towards an all-optical control of the information [1]. Thus, the active control of the timing of light pulses is attracting much attention for the development of fast-access memories and optically-controlled delay lines compatible with fibre-optic communication systems. It is possible to achieve a control of the speed of light by creating spectrally narrow gain/loss bands in the medium through optical pumping. In this kind of steep transitions, the group index is strongly increased or reduced, giving as a result that the group velocity (i.e. the velocity at which a narrowband signal propagates) is strongly modified [2]. This effect had only been observed in the resonances of certain ultracold atomic gases through a process called electromagnetically-induced transparency (EIT) [3] and in certain crystalline solids using the process known as population oscillations (PO) [4]. However, these demonstrations were performed at wavelengths of little interest for fiber-based optical

communications. Additionally, several techniques to achieve slow and fast light have been demonstrated in optical fibers, namely using stimulated Brillouin [5], Raman scattering [6] and parametric amplification [7]. All these embryonic studies show clearly the strong potential of this way of implementing optically-controlled delay lines.

The demonstration of the slow light effect in AlGaAs/GaAs multiple quantum wells (MQW) at 850 nm wavelength using the PO technique [8] has paved the way for achieving similar results in the wavelength band of interest for optical fibers (1.3-1.5 μm) by using suitably band-engineered materials. In particular, InN and ternary semiconductors based on GaN and InN are ideal candidates, since they exhibit direct bandgap and a highly stable behaviour. Also, quantum wells and quantum dots with high In content and InGaN or GaN barriers should allow meeting the required wavelengths. Furthermore, absorption saturation processes in InN have been reported [9,10], which is a requirement for slow light generation in solids.

This paper presents a preliminary evaluation on the suitability of InN for the development of slow light devices in the spectral region around 1.5 μm. To this aim, we have measured the third-order susceptibility, $\chi^{(3)}$, of thick InN samples with different apparent optical band-gap. With this data, we have calculated the slow-down factor that we can achieve in the material at reasonable pump fluencies, reaching values in the order of 4.2. Estimations of *S* factor for InN/InGaN shows that further work in these heterostructures may yield slow down factors several orders of magnitude higher.

2. Experimental results.

The InN samples investigated in this work were grown on 10-μm-thick non-intentionally-doped (nid) GaN-on-sapphire templates and on Si(111) substrates by

plasma-assisted molecular beam epitaxy (PAMBE). In-situ growth monitoring was performed by Reflection High Energy Electron Diffraction (RHEED).

In the case of the InN grown on GaN-on-sapphire templates (sample S1), prior to the growth of the InN layer, a 10-nm-thick nid GaN buffer layer was deposited at 720 °C. InN growth was then carried out at a substrate temperature of 450 °C, with a N flux corresponding to a growth rate of 0.3 monolayers per second, and with an In/N ratio of 1.2. Periodic growth interruptions under N are performed to consume the In excess and prevent the accumulation of In droplets on the surface. The growth period (InN growth time / growth interruption time) for sample S1 was 5 min / 1 min.

For InN sample grown on Si(111) (sample S2), the substrates were heated in the growth chamber at 800 ºC for 30 minutes to remove the native oxide. The AlN buffered Si(111) was preceded by depositing a few monolayers of metallic Al at high temperature. Afterwards, the AlN buffer layer was grown at 780ºC at a rate of 200 nm/hour to minimize surface roughness [11]. Once the buffer layer is grown, the growth is stopped to decrease the temperature down to 475 ºC [12]. InN layers were grown under slightly indium rich conditions at a rate of 0.8 µm/hour. A streaky 1x1 RHEED pattern observed during all the growth indicates two-dimensional growth mode.

Linear optical properties of the samples in the wavelength range of 1100–2550 nm were studied at room temperature by normal-incidence transmission measurements, using a Perkin-Elmer Lambda 9 scanning spectrophotometer.

Optical non linear characterization has been performed by forward degenerate four-wave mixing (DFWM) technique in boxcars configuration [13]. For this technique, the excitation source used was an optical parametric amplifier (OPA) providing 100 fs pulses, tunable in the 300–3000 nm interval, at a repetition rate of 1 kHz. The relaxation

time of the excited carrier population grating (τ) has been determined by introducing a delay line in one of the arms of the experimental setup.

Figure 1 shows the measured transmission data (straight line) of the investigated InN samples. Substrate limits the maximum transmittance to 0.86 and 0.53 for sapphire and silicon, respectively. Experimental transmission spectra were compared with theoretical calculations using a three layer model (substrate/buffer layer/InN) [14] to obtain values of thickness, ordinary refractive index $n_0(\lambda)$, and absorption coefficient $\alpha(\lambda)$ of the InN layer. A sigmoidal approximation was used for $\alpha(\lambda)$ [15], meanwhile $n_0(\lambda)$ was obtained in the transparency region considering a first order Sellmeier dispersion formulas[16]. Scattering from rough surface is included in the calculations follow the model proposed by Filinski [17]. The optical absorption band edge of the samples is estimated at 1550 nm (sample S1) and 1650 nm (sample S2). High Resolution X-Ray diffraction measurements (not shown) lead to values of c-lattice parameter of 5.690 Å (S1) and 5.700 Å (S2), within the range of values measured in high quality single crystalline InN films (scattered in the range of c = 5.69-5.705 Å [18]). Thus, the difference in the obtained optical band gap is attributed to the Burstein-Moss effect induced by a slightly different residual electron concentration in the samples, both in the range of 10^{19} cm^{-3} [19].

Table I summarizes the linear optical estimations performed for 1500 nm applied to the later $|\chi^{(3)}|$ calculation. Absorption by the GaN and AlN buffer layers (sample S1 and S2, respectively) was considered negligible at 1500 nm, while refractive index of GaN and AlN was estimated about 2.23 and 1.75 at 1500 nm, respectively.

Regarding the DFWM measurements, the coefficient c of the relationship $I_C = cI_P^3$ has been obtained by plotting the conjugated beam intensity I_c versus the pump intensity I_p. A fused silica (SiO_2) plate with $|\chi^{(3)}|$=1.28 x 10^{-14} esu and n_0=1.45

[13] was used as reference. Details about $|\chi^{(3)}|$ calculations can be found in ref. [20]. $|\chi^{(3)}|$ values of (5.4±0.6)x 10^{-10} and (8.0±0.8)x 10^{-10} esu were measured at 1500 nm for samples S1 and S2, respectively. The obtained $|\chi^{(3)}|$ value increases with the linear absorption of the samples, being higher for the sample with the lowest optical bandgap (S2). This behavior is consistent with a resonant excitation, as observed when analyzing the change in $|\chi^{(3)}|$ with the excitation wavelength for a given sample [20].

The resonant character of the involved mechanism for InN leads to values of $|\chi^{(3)}|$ close to two orders of magnitude above the measured for GaN (4.4±0.4)x10^{-12} esu [20] and Si 2.8x10^{-11} esu [21] at 1500 nm. Furthermore, contribution of substrate to the measured $|\chi^{(3)}|$ was neglected performing the DFWM experiments with a pump power below the limit to obtain a measurable nonlinear response for the substrate [20].

Figure 2 shows the DFWM signal intensity as a function of the induced delay time for the analyzed samples. Lifetime estimated for sample S1, with a band gap closer to excitation wavelength is of 4.8 ps. This lifetime is attributed to a non-radiative recombination mechanism, related to the defects responsible of the free carrier concentration of the layers, in the range of ~10^{19} cm^{-3} [10]. This time is comparable to the lifetime of 12 ps obtained in GaAs quantum-dot-based optical amplifiers, used to obtain room temperature slow and fast light [22].

In case of sample S2 which shows lower bandgap energy, the estimated lifetime is of 0.8 ps being attributed to relaxation of hot carriers from higher energy states to lower energy states [9].

3. Slow-down factor estimations.

In this section, we analyse the suitability of InN for all-optical control of light speed applications at 1.5 μm by obtaining the *S* factor, for samples S1 and S2.

The obtained values of $|\chi^{(3)}|$ and τ were used to calculate the nonlinear absorption coefficient, α_2, of the samples following the equation [23]:

$$\alpha_2 = \frac{3\upsilon_0 \,\mathrm{Im}\left(\chi^{(3)}\right)}{2\varepsilon_0 n_0^2 c^2} \qquad (1)$$

, where n_0 and ν_0 are the linear refractive index and the resonance frequency (200 THz), respectively. The imaginary part of $|\chi^{(3)}|$ was considered to be of the same order of magnitude of $|\chi^{(3)}|$. Values of α_2 of -24 cm/GW and -34 cm/GW were obtained for samples S1 and S2, respectively. These values are similar to the ones obtained in GaN layers for close to the bandgap wavelengths (in the order of -20 cm/GW [24]). The observation of absorption saturation in these materials [11] provides a further confirmation of the negative sign of α_2.

The calculated non-linearly induced dip in absorption, estimated considering a Lorentzian-type lineshape, is shown in the inset of fig. 2. The Full Width at Half Maximum (FWHM) bandwidth, $\Delta\nu$ is calculated as the inverse of the measured lifetime of the population grating [23], leading to values of 66 GHz and 398 GHz for sample S1 and S2, respectively. This line shape leads to a phase-change of the wave travelling across the sample of [25]:

$$\phi = L_{eff}\frac{\alpha_2 I}{2}\frac{\left(\nu-\nu_0 \big/ (\Delta\upsilon/2)\right)}{1+\left(\nu-\nu_0 \big/ (\Delta\upsilon/2)\right)^2} \qquad (2)$$

, where the linear absorption of the sample, which reduce the nonlinear effects when increasing the sample depth, is introduced through the effective length, calculated by $L_{eff} = (1-e^{\alpha z})\big/\alpha$. The S factor of the samples is then obtained by $S(\nu) = \left(c \big/ 2\pi z\right) d\phi \big/ d\nu$. Figure 3 shows the S factor obtained, considering a sample thickness of 1 μm and a typical pump intensity of 3 GW/cm^2. Maximum values of S of

4.2 and 0.7 were obtained for samples S1 and S2, respectively. The estimated value of *S* decreases when considering the linear absorption, as expected due to a decrease of the pump intensity along the sample (see figure 3). The lower slow-down factor obtained for sample S2, is related to its higher linear absorption at the analyzed wavelength.

The values of *S* could be enhanced by using low dimensional heterostructures, where both the nonlinear parameters [26] and the carrier lifetime [27] increases. The band structure of an InN/InGaN-based MQW was calculated from 1D self-consistent simulations using Nextnano^3 software [28]. The MQW structure was simulated to obtain transition between the first confined level of electron and holes in the QWs at 1500 nm. The inset in figure 3 shows an estimation of the *S* factor for a 20-periods of the resultant structure, InN (5 nm)/$In_{0.7}Ga_{0.3}N$ (8 nm) MQW. Taking into account a value of $|\chi^{(3)}|\sim10^{-8}$ esu, and $\tau \sim 0.1$ ns (100 times higher [26] and 20 times higher [27] than the values for bulk material, respectively) a *S* factor up to 10000 was estimated. This value is in the order of the obtained one of 30000 for GaAs/AlGaAs heterstructures used for optically controlled speed of light at 830 nm [8]. This would open the possibility of using InN-based heterostructures for slow-light applications.

4. Conclusions.

In this work, we have evaluated the capability of InN for optically controlling the speed of light at 1500 nm. DFWM measurements point out a resonance character of $|\chi^{(3)}|$ as corresponds to close to band gap transitions. Values of $|\chi^{(3)}|$ in the range of 10^{-10} esu were obtained for wavelengths close to (below 150 nm) the optical bandgap. Recombination time of the induced population grating decreases when increasing the difference between excitation and optical band gap wavelength, from 4.7 ps to 0.8 ps. This difference is attributed to changing in relaxation mechanism, from no radiative

band to band relaxation (long time) to hot carrier relaxation (short time). *S* factor increases when decreasing the difference between excitation wavelength and optical bandgap, due to a decrease in linear absorption, and an increase of the population grating lifetime. Maximum *S* factor of 4.2 was obtained in that case, for a pump intensity of 3 GW/cm^2. Simulations performed for InN-based quantum well structures show that this *S* factor could be increased to 10000 due to the increase of $|\chi^{(3)}|$ and τ. Nevertheless, the obtaining of this S factor depends on the achievement of high quality material to allow excitonic nonlinearities. These results would open the possibility of using InN-based heterostructures for slow-light applications.

Acknowledgements

Partial financial support was provided by Spanish government projects TEC2006-09990-C02-02/TCM, TEC2005-00074/MIC and HF2007-0065.

References

[1] D. A. Fishman, Y. -H. Kao, X. Liu, and S. Chandrasekhar, J. Opt. Netw. 7, (2008) 310.

[2] R. W. Boyd and D. J. Gauthier, Progress in Optics 43, (2002) 497.

[3] L. V. Hau, S. E. Harris, Z. Dutton and C. H. Behroozi, Nature 397, (1999) 594.

[4] M. S. Bigelow, N. N. Lepeshkin and R. W. Boyd, Science 301, (2003) 200.

[5] M. Gonzalez-Herraez, K. Y. Song and L. Thevenaz, Appl. Phys. Lett. 87 (2005) 08113.

[6] J. E. Sharping, Y. Okawachi and A. L. Gaeta, Opt. Express 13, (2005) 6092.

[7] D. Dahan and G. Eisenstein, Opt. Express 13, (2005) 6234.

[8] P. C. Ku, F. Sedwigck, C. J. Chang-Hasnain, P. Palinginis, H. L. Wang, T. Li, S. W. Chang and S. L. Chuang, Opt. Lett. 29, (2005) 2291.

[9] F. Chen, A. N. Cartwright, H. Lu, W. J. Schaff, J. Cryst. Growth 269, (2004) 10.

[10] F. Chen, A. N. Cartwright, H. Lu, J. Schaff, Appl. Phys. Lett. 83, (2003) 4984.

[11] E. Calleja, M.A. Sánchez-García, F.J. Sánchez, F. Calle, F.B. Naranjo, E. Muñoz, S.I. Molina, A.M. Sánchez, F.J. Pacheco and R. García, J. Crys.Growth 201/202, (1999) 296.

[12] J.Grandal and M.A.Sánchez-García, J. Crys. Growth, 278, (2005) 373.

[13] R.L. Sutherland, "Handbook of nonlinear optics" Marcel Dekker, Inc., New York (1996).

[14] M.J. Bergman, Ü. Özgür, H.C. Casey, J.F. Muth, Y.C. Chang, R.M.Kolbas, R.A. Rao, C.B Eom, and M. Schurman, Appl. Phys. Lett. 74, (1999) 3188.

[15] F.B. Naranjo, M.A. Sánchez-García, F. Calle, E. Calleja, B. Jenichen, and K.H. Ploog, Appl. Phys. Lett. 80, (2002) 231.

[16] N. Antoine-Vincent, F. Natali, M. Mihailovic, A. Vasson, J. Leymarie, P. Disseix, D. Byrne, F. Semond, and J. Massies, J. Appl. Phys. 93, (2003) 5222.

[17] Z. Yin, H.S. Tan, F.W. Smith, Diam. Relat. Mater. 5 (1996) 1490.

[18] A. G. Bhuiyan, A. Hashimoto, A. Yamamoto, J. Appl. Lett. 94, (2003) 2779.

[19] K. S. A. Butcher, T.L. Tansley, Superlatt. and Micros. 38, (2005) 1.

[20] F.B. Naranjo, M. González-Herráez, H. Fernández, J. Solis, E. Monroy, Appl. Phys. Lett. 90, (2007) 091903.

[21] D. Dimitropoulos, V. Raghunathan, R. Claps, and B. Jalali, Opt. Exp. 12, (2004) 149.

[22] H. Su, and S.L. Chuang, Appl. Phys. Lett. 88, (2006) 061102.

[23] M. Sheik-Bahae, M. P. Hasselbeck, "Third Order Optical nonlinearities" OSA Handbook of Optics, Vol IV. Chapter 12. (2000).

[24] Y.-L. Huang, C.-K. Sun, J.-C. Liang, S. Keller, M.P. Mack, U.K. Mishra, and S.P. DenBaars, Appl. Phys. Lett. 75 (1999) 3524.

[25] L. Thévenaz, K. Y. Song, M. González-Herráez, Opt. Lett. 31, (2006) 715.

[26] K. D. Choquette, L. McCaughan, D.K. Misemer, J. Appl. Phys. 66, (1989) 4387.

[27] A. Sasaki, K. Nishizuka, T. Wang, S. Sakai, A. Kaneta, Y. Kawakami, Sg. Fujita, Solid Stat. Comm. 129, (2004) 31.

[28] Nextnano[3]. Available on-line: **http://www.nextnano.de**

Table I: Summary of results obtained from linear and non-linear optical measurements at 1500 nm.

Sample	Substrate	Thickness (nm)	α (cm^{-1})	n	αL	$\lvert\chi^{(3)}\rvert$ (esu)
S1	GaN template	650	4.7×10^{3}	2.85	0.3	$5.4 \pm 0.5 \times 10^{-10}$
S2	Si(111)	1000	1.2×10^{4}	2.95	1.3	$8.0 \pm 0.8 \times 10^{-10}$

Table I. F.B. Naranjo *et al*.

Figure captions.

Figure 1. Transmission spectra of the InN analyzed samples. Inset: Calculated absorption coefficient.

Figure 2. DFWM signal intensity obtained as a function of delay time between one of the pumps and the others for the samples S1 and S2. Inset: Calculated absorption for the analyzed samples as a function of detuning, for pump intensity of 3 GW/cm^2.

Figure 3. *S* factor of analyzed InN samples at 1500 nm as a function of detuning, considering excitation pump power of 3 GW/cm^2 and 1 μm sample thickness. Inset: Calculated *S* factor for a InN (5 nm)/$In_{0.7}Ga_{0.3}N$ (8 nm) MQW with 1500 nm of resonance wavelength.

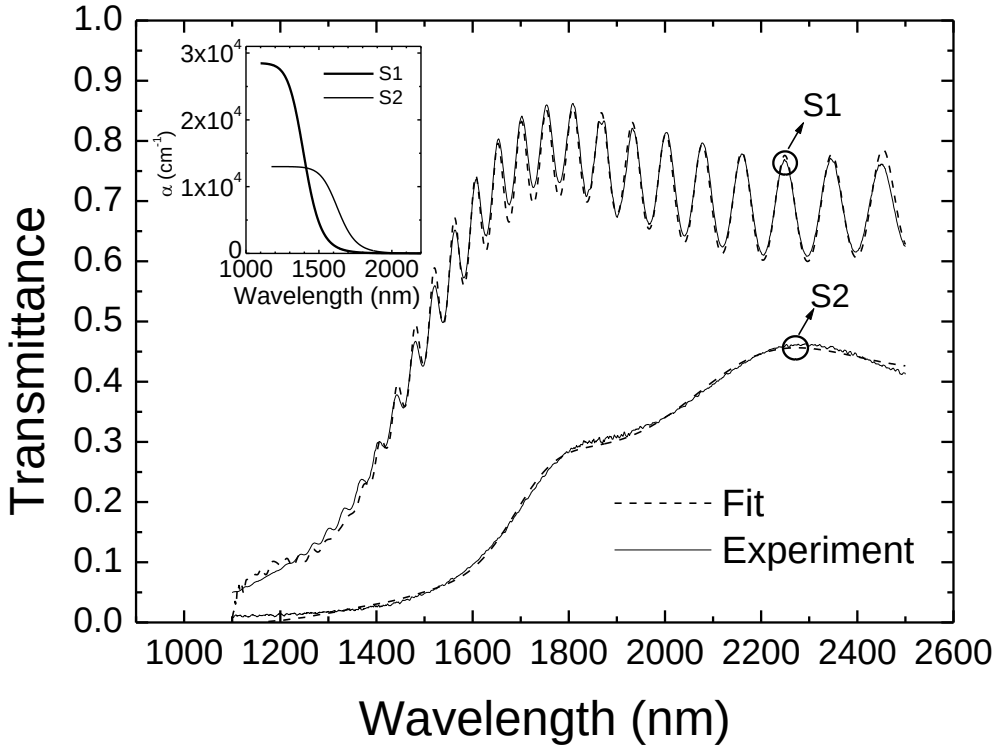

Figure 1. F.B. Naranjo *et al*.

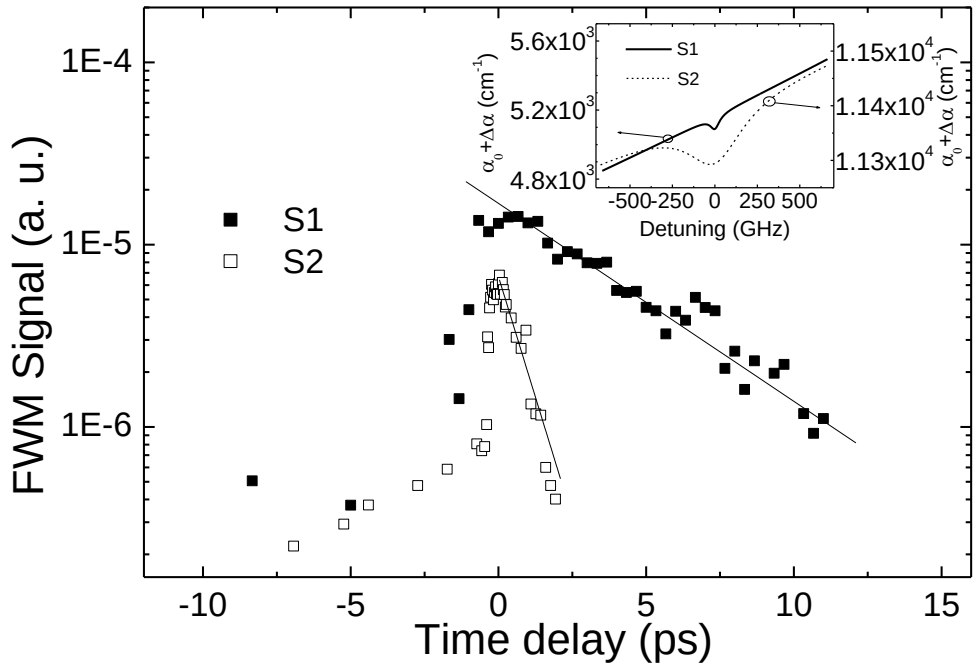

Figure 2. F.B. Naranjo *et al*.

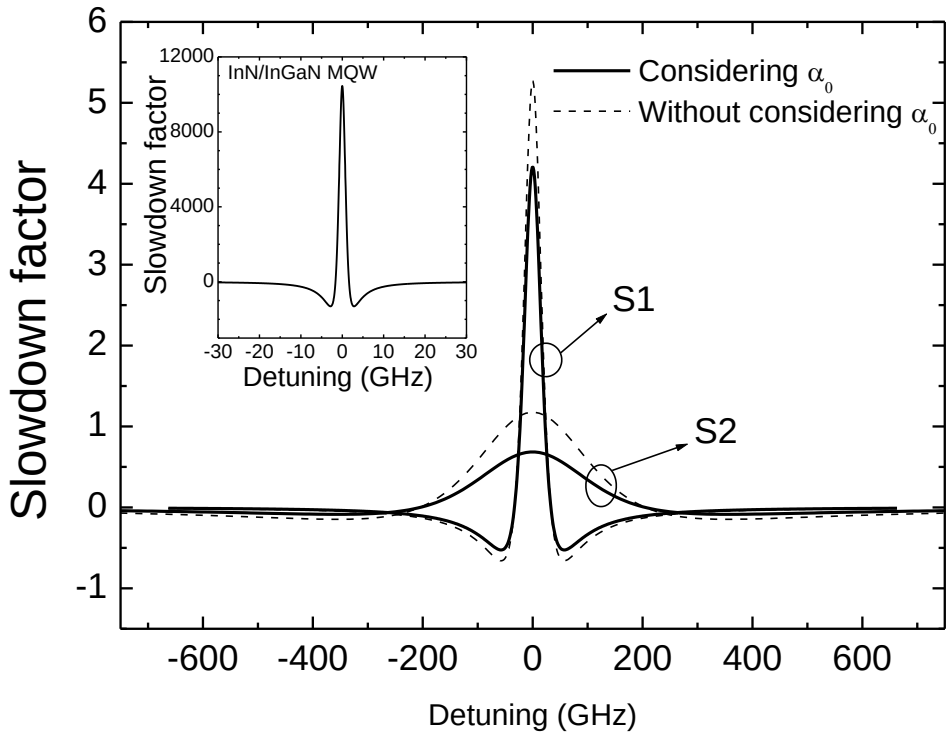

Figure 3. F.B. Naranjo *et al*.